Article

Cite This: *Biomacromolecules* 2018, 19, 3861−3873

pubs.acs.org/Biomac

Tunability of Biodegradable Poly(amine-*co*-ester) Polymers for Customized Nucleic Acid Delivery and Other Biomedical Applications

Amy C. Kauffman,[†,⊥] Alexandra S. Piotrowski-Daspit,[†,⊥] Kay H. Nakazawa,[†] Yuhang Jiang,[†] Amit Datye,[‡] and W. Mark Saltzman*[,†,§,∥]

[†]Department of Biomedical Engineering, [‡]Department of Mechanical Engineering and Materials Science, [§]Department of Chemical & Environmental Engineering, and [∥]Department of Physiology, Yale University, New Haven, Connecticut 06511, United States

Supporting Information

ABSTRACT: Gene therapy promises to treat diseases that arise from genetic abnormalities by correcting the underlying cause of the disease rather than treating the associated symptoms. Successful transfer of nucleic acids into cells requires efficient delivery vehicles that protect the cargo and can penetrate the appropriate cellular barriers before releasing their contents. Many viral vectors and synthetic polycationic vectors for nucleic acid delivery do not translate well from *in vitro* to *in vivo* applications due to their instability and toxicity. We synthesized and characterized a library of biocompatible low charge density polymers from a family of poly(amine-*co*-ester) (PACE) terpolymers produced via enzyme catalyzed polymerization. PACE polymers are highly customizable; we found that the terpolymer composition can be optimized to produce efficient transfection of various nucleic acids—including DNA plasmids, mRNA, and siRNA—in specific cell types with low toxicity. Our findings suggest that the unique tunability of PACEs offers new tools for gene therapy and other biomedical applications.

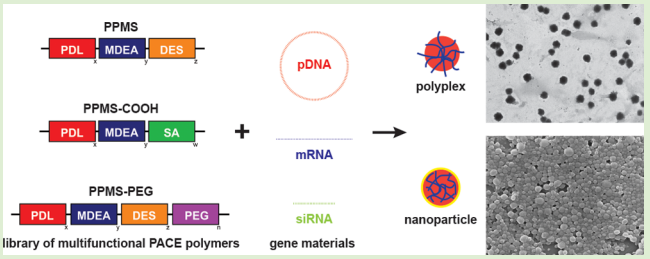

INTRODUCTION

The controlled modification of gene expression via the delivery of nucleic acids is becoming an increasingly promising approach for treatment of disorders that arise from genetic abnormalities in modern medicine as well as for genetic manipulation in basic research. Both viral and non-viral methods have been utilized for delivery of genetic material.[1] While viral delivery can be highly efficient, recombinant viral vectors in therapeutic applications are often immunogenic and cytotoxic.[2] Lipid or polymeric vehicles, on the other hand, tend to be less toxic and can be engineered to successfully transfer a variety of types and sizes of nucleic acids, including DNA, mRNA, siRNA, and miRNA.[3,4] Biodegradable cationic polymers are particularly promising for the delivery of negatively charged nucleic acids.[5] Delivery vehicles formulated with such polymers will ideally form favorable electrostatic interactions with their cargo and protect it from degradation and elimination. Cationic polymers can also mediate cellular uptake by interactions with the negatively charged phospholipid membrane[6] and can be designed to dissociate in the intracellular environment.[7] To achieve optimal efficacy, polymer design is critical. Characteristics of the polymer—such as chemical composition, hydrophobicity, thermal properties, and molecular weight—will determine the physical characteristics of the resulting delivery vehicle. Further, the choice of formulation protocol used to generate the delivery vehicles from raw polymer materials will dictate important features of the vehicles themselves, including size, morphology, surface charge, stability, cargo loading efficiency, and kinetics of nucleic acid release. All of these parameters potentially contribute to the effectiveness and safety of the resulting nanomaterial.

Many cationic polymers developed thus far exhibit significant cytotoxicity in cell-based assays or animal models due to excess charge density, which can disrupt vital cellular processes.[8] Polyethylenimine (PEI), for example, is a cationic polymer composed of repeating units of an amine group and two carbon aliphatic spacers, and readily complexes with nucleic acids.[9,10] While high efficacy in transfection is achieved, PEI exhibits significant toxicity by cell or mitochondrial membrane disruption leading to necrosis or apoptosis.[11−13] Reducing the charge density of such cationic polymers, by manipulations such as decreasing the molecular weight or including additional chemical moieties into the polymer chain, have been shown to decrease cytotoxicity.[14,15] However, lower molecular weight variants of PEI are less effective as transfection agents.[14] The synthesis of cationic polymers with lower charge densities, but adequate molecular weights, could

Received: June 26, 2018
Revised: August 14, 2018
Published: August 15, 2018

DOI: 10.1021/acs.biomac.8b00997
Biomacromolecules 2018, 19, 3861−3873

fulfill unmet needs in the application of transfection agents. Moreover, branched polymers, including branched PEIs, tend to have high chain mobility and little to no crystalline structure (i.e., they are amorphous) leading them to be liquids at all molecular weights at physiologically relevant and formulation/processing temperatures.[16] Thus, these polymers can only be formulated into transient delivery vehicles (such as polyplexes) that lack the stability needed for most clinical applications. Further, it is difficult to engineer polyplexes that provide controlled and sustained cargo release.

We have developed a versatile family of mildly cationic poly(amine-*co*-ester) (PACE) polymers, some of which have already shown significant promise for the delivery of nucleic acids such as plasmid DNA, microRNA, mRNA, and siRNA.[5,17−19] In these prior studies, different members selected from the PACE family of polymers have shown high nucleic acid loading, sustained or short-term cargo release, and high biocompatibility. This prior work has not examined a wide range of PACE compositions, nor identified correlations between properties of the polymer and biological activity.

Here, we expand the PACE family of polymers by modifying chemical compositions, generating three subsets of poly(pentadecalactone-*co*-*N*-methyldiethanolamine-*co*-sebacate) (PPMS) that have previously been reported:[5,17] PPMS, PPMS with a carboxyl end group (PPMS-COOH), and a block copolymer of PPMS and poly(ethylene glycol) (PPMS-PEG). These modifications result in new customizable formulations with unique physiochemical characteristics, while maintaining biocompatibility. We also demonstrate the ability of these new formulations to be successfully formulated into delivery vehicles and transfect genetic materials into multiple human and animal cell types. PACE polymers are synthesized in small batches via enzymatic copolymerization of diesters with amino-substituted diols and a lactone. The most commonly used PACE polymer, PPMS, is composed of: a lactone that confers hydrophobicity and reduces cytotoxicity, an amino-diol that provides a mildly cationic charge via a tertiary amine, and a long chain diester that enables additional hydrophobic control. Alterations in end group chemistry of the polymers can be achieved by selection of the appropriate diester ultimately leading to altered chemical functionalities. For example, substituting sebacic acid for diethyl sebacate yields a polymer with a carboxylic acid end group providing opportunities for conjugation. Further, additional customization can be achieved by controlling the molar feed ratios of the monomers. Altering monomer ratios can result in control over molecular weight, hydrophobicity, and nitrogen content. For example, an increase in the lactone content results in the synthesis of polymers with diverse chemical, physical, and thermal properties.

The unique characteristics of PACE polymers can lead to the development of a wide array of delivery vehicles that are efficient at both encapsulating nucleic acid cargo and delivering these agents to target cells. The mildly cationic charge of PACE polymers is likely to improve association with cells and promote the release of nucleic acid cargo compared to polymers with higher charge densities. Moreover, molecular weight and hydrophobicity can also improve delivery; higher molecular weight polymers are more efficient in condensing with nucleic acid cargo,[20] and hydrophobic domains enhance delivery vehicle stability and facilitate cargo release.[21] Lastly, customization of physical, thermal, and mechanical properties via monomer selection and co-monomer ratio can open new avenues of use for PACE family polymers beyond transfection agents, for example, as components of medical devices and structures in the form of scaffolds or films or implants. Here we elucidate the unique ability of this family of polymers to promote high cellular uptake and efficiently deliver plasmid DNA (pDNA), mRNA, and siRNA.

EXPERIMENTAL SECTION

Materials. 15-Pentadecalactone (PDL, 98%), diethyl sebacate (DES, 98%), sebacic acid (SA, 98%), *N*-methyldiethanolamine (MDEA, 99+%), polyethylene glycol (PEG, 5000 MW), diphenyl ether (99%), immobilized *Candida antarctica* lipase B (CALB) supported on Novozym 435, chloroform (HPLC grade), chloroform-*d* (NMR grade), dichloromethane (HPLC grade, 99+%), hexanes (HPLC grade, 97+%), and methanol (98%) were all purchased from Sigma-Aldrich and used as received.

Synthesis and Purification of PACE Polymers. Three variants of the PACE polymer poly(pentadecalactone-*co*-*N*-methyldiethanolamine-*co*-sebacate) (PPMS) were synthesized as described previously with some modification.[5] Briefly, copolymerization of a lactone with an amino-substituted diol and a diester was performed in diphenyl ether via enzyme catalyst (CALB) using a Schlenk line connected to a vacuum line with the vacuum controlled by a digital vacuum regulator. In the first stage (oligomerization) the reactants and solvent were stirred at 250 rpm at 90 °C under 1 atm of argon gas for 20 h. In the second stage (polymerization), the reaction was continued for an additional 48 h with the system pressure reduced to 2.5 mmHg. The resulting crude polymer was then washed in hexane three times, dissolved in dichloromethane or chloroform, and filtered. The added dichloromethane or chloroform was then removed via a rotary evaporator. The polymer was stored in an airtight, sealed vessel in a desiccator box at −20 °C until needed.

Chemical Structure Analysis of Polymers. To confirm polymer composition, proton nuclear magnetic resonance (^{1}H NMR) was used. Polymer samples were dissolved in chloroform-*d* and analyzed via an Agilent DD2 400 MHz NMR spectrometer equipped with a two-channel system, an AS7620 96-sample changer, and a OneNMR probe with auto-tune-and-match installed (Agilent, Santa Clara, CA, USA). Spectra were analyzed via MestraNOVA software where manual peak assignment was used, and manual integration was used to quantify post-synthesis monomer content (Mestralab Research, S.L., Santiago de Compostela, Spain).

Molecular Weight Determination Polymers. The number- and weight-average molecular weights of all polymers were measured by gel permeation chromatography (GPC) driven by the Ultimate 3000 UHPLC system (Thermo Fisher Scientific, Waltham, MA, USA) equipped with a TREX refractive index detector (Wyatt Technologies, Santa Barbara, CA, USA). The instrument was controlled using Chromeleon 7.2 Chromatography Data System software (Thermo Fisher Scientific, Waltham, MA, USA) and data collection and analysis was performed in ASTRA 6.0 (Wyatt Technologies, Santa Barbara, CA, USA).

Polymer Thermal Property Assessment. A small aliquot of polymer was measured into a TZero aluminum pan or Hermetic aluminum pan, sealed, and analyzed via a Q20 differential scanning calorimeter (DSC) (TA Instruments, New Castle, DE, USA). Polymer samples with molar PDL content less than or equal to 40% were equilibrated at −70 °C, ramped to 0 °C at 10 °C/min, held isothermal for 1 min then cooled to −70 °C at 10 °C/min. Polymer samples with molar PDL content equal or greater than 50% were equilibrated at 10 °C, ramped to 90 °C at 10 °C/min, held isothermal for 1 min then cooled to 10 °C at 10 °C/min. Heating curves were analyzed via TA Universal Analysis software (TA Instruments, New Castle, DE, USA).

Contact Angle Determination on Polymer Thin Films. The wettability of solvent-casted polymer thin films was measured via the sessile drop method utilizing a contact angle goniometer (Attension Theta, Biolin Scientific, Västra Frölunda, Sweden). Briefly, a 2 μL droplet of water was placed on the surface of the film and the droplet

DOI: 10.1021/acs.biomac.8b00997
Biomacromolecules 2018, 19, 3861−3873

relaxation was captured at 6 frames per second for 20 s with a high-speed camera. The contact angle was then analyzed using Attension One software (Biolin Scientific, Västra Frölunda, Sweden).

Polyplex and NP Formulation and Characterization. PPMS polymers were formulated into either polyplexes or solid nanoparticles (NPs); low PDL content polymers (10−20 mol%) were formulated as polyplexes and higher PDL content polymers (50−80 mol%) polymers were formulated as solid NPs. Nucleic acid polyplexes with a weight ratio of 100:1 polymer:nucleic acid were used for all *in vitro* studies. Polymers were dissolved at 100 mg/mL in DMSO overnight and then diluted in sodium acetate buffer (25 mM, pH 5.8) and vortexed for 15 s. Nucleic acids were similarly diluted in sodium acetate buffer. The polymer solution was then added to the nucleic acid solution and the mixture was vortexed for 25 s and then incubated at room temperature for 10 min before treating cells. Control Lipofectamine 2000, Lipofectamine 3000, Lipofectamine RNAiMAX, and TransIT (Mirius) transfection agents were used as respective controls according to the protocols provided by the manufacturers. For polyplex uptake experiments, a short 19-bp duplex DNA strand with a 5′ Cy5 fluorescent tag was used as the nucleic acid cargo.

Solid NPs were formulated using a modified single oil-in-water (o/w) or double water-in-oil-in-water (w/o/w) emulsion solvent evaporation technique as previously described.[22] Briefly, 50 mg of polymer was dissolved in 1 mL of dichloromethane or chloroform overnight. For DiO-loaded formulations, 0.2 wt% of dye to polymer was used. Immediately prior to formulation, 10 μL of dye (10 mg/mL in DMSO) was added to the dissolved polymer. This solution was then added dropwise under vortex into 2 mL of 5 wt% low-molecular-weight poly(vinyl alcohol) (PVA) solution and sonicated to form an oil-in-water single emulsion. For nucleic acid-loaded formulations, the nucleic acid cargo was first dissolved in sodium acetate buffer (25 mM, pH 5.8) and added dropwise under vortex into the dissolved polymer solution and sonicated using a probe tip sonicator three times for 10 s to form the first water-in-oil emulsion. This emulsion was then added dropwise under vortex into 2 mL of 5% low molecular weight PVA solution and sonicated to form the water-in-oil-in-water double emulsion. Both single and double emulsions were then diluted into 10 mL of 0.3% PVA solution while mixing and then transferred to a round-bottom flask. The particle solution was then placed on the rotary evaporator for 15 min to remove the dichloromethane. The NPs were then washed twice in pure water by centrifugation. Particles were resuspended with 30 mg trehalose, lyophilized for least 48 h, and stored at −20 °C. The size and zeta potential of freshly prepared polyplexes and NPs were measured using dynamic light scattering (Zetasizer Pro, Malvern Panalytical, Malvern, United Kingdom). The morphologies of polyplexes were visualized using tungsten stain via transmission electron microscopy (TEM). The morphologies of solid NPs were visualized using gold palladium coating via scanning electron microscopy (SEM). Nucleic acid loading of solid NPs was measured using QuantIT PicoGreen (pDNA) or RiboGreen (mRNA, siRNA) assays. Briefly, 2 mg of particles were dissolved in 700 μL of dichloromethane and shaken at 37 °C overnight. Next, 500 μL of TE buffer was added to the samples, which were vortexed and placed on a shaker incubator for 30 min. Samples were then centrifuged for 5 min at 15000*g*, and the aqueous phase was extracted. A second extraction was performed, and the total aqueous extract was used for the QuantIT PicoGreen or Ribogreen assay according to manufacturer protocols. Cumulative nucleic acid release from solid NPs was characterized by dissolving 0.5−1 mg of NPs in 0.5 mL of DPBS and adding this solution into Slide-A-Lyzer mini dialysis devices (MW cutoff 10 kDa), which were placed in microcentrifuge tubes containing 1.5 mL of DPBS. These tubes were then placed in a shaking incubator at 37 °C. At each time point, the DPBS in the microcentrifuge tubes containing released nucleic acid was collected, and 1.5 mL of fresh DPBS was added to the tubes. Nucleic acid concentrations in the collected solutions were then quantified using QuantIT PicoGreen or RiboGreen assays.

Cell Culture. Human embryonic kidney 293 (HEK293, ATCC) and A549 human lung cancer cells (ATCC) were cultured in 1:1 Dulbecco's modified Eagle's medium (DMEM)/F12 medium supplemented with 10% fetal bovine serum (Atlanta Biologicals) and 50 μg/mL gentamicin. Human dermal fibroblasts (HDF, ATCC) were cultured using the Fibroblast Growth Kit-Low serum (ATCC) supplemented with penicillin (10 000 units)−streptomycin (10 mg)−amphotericin B (25 μg). NIH 3T3 mouse fibroblasts (ATCC) were cultured in 1:1 high glucose DMEM supplemented with 10% bovine calf serum (BCS) and penicillin (10 000 units)−streptomycin (10 mg). Cells were maintained in a 37 °C incubator under a humid 5% CO_2 atmosphere.

Polyplex and NP Biocompatibility and Uptake Assessment *in Vitro*. Biocompatibility of polyplexes and NPs was assessed using a neutral red assay as previously described.[23] Briefly, 100 μL cells were seeded in a 96-well tissue culture treated plates at approximately 50 000 cells/mL. Cells were exposed to polyplexes or NPs in a concentration range from 0.05 to 1.0 mg/mL in their respective media for 24 h, and washed with PBS, after which the neutral red media and destaining protocol was followed. Absorbance was measured using a plate reader at 540 nm with 850 nm background subtraction.

To determine the extent of NP uptake into cultured cells, cells were seeded in 24-well tissue culture plates at a density of 100 000 cells/well (or 50 000 cells/well in the case of A549 cells) in 500 μL of culture medium 24 h before polyplex or NP treatment. Cells in each well were then treated with polyplexes complexed with a total of 1 μg of a short 19-bp duplex scrambled DNA (IDT) with a 5′ Cy5 fluorescent tag or DiO-loaded solid NPs at a concentration of 0.1 mg/mL. Uptake of fluorescent polyplexes or solid NPs was quantified using flow cytometry (Attune NxT, Life Technologies, Carlsbad, CA, USA). Briefly, cells were washed three times with PBS 24 h after treatment, harvested, and washed again in 2% BSA in PBS prior to analysis. All results were analyzed using FlowJo software (FlowJo LLC, Ashland, OR, USA). Uptake was further confirmed using fluorescence microscopy. In this case, treated cells were fixed in 4% paraformaldehyde for 15 min and then stained with Hoechst 33342 (Tocris Bioscience, Bristol, United Kingdom). Samples were then permeabilized in 0.3% Triton X-100 (Sigma-Aldrich, St. Louis, MO, USA) in 2% BSA for 30 min and incubated in Alexa Fluor 594 phalloidin (Thermo Fisher, Waltham, MA, USA) for 20 min per the manufacturer's instructions. All samples were imaged via fluorescence microscopy (Olympus IX71, Tokyo, Japan).

pDNA, mRNA, and siRNA Transfection Assessment. The delivery of pDNA, mRNA, and siRNA by PACE polyplexes and NPs was assessed in HEK293 cells and compared to commercial transfection methods and the delivery of nucleic acids in the absence of transfection agents. Cells were seeded at 100 000 cells/well in a 24-well plate in 500 μL of culture medium 24 h prior to treatment for all studies. A pcDNA3-EGFP plasmid (Addgene 13031) was used for pDNA studies, EGFP mRNA (TriLink L-7201-100) was used for mRNA studies, and siRNA against BIRC5 (Survivin, Dharmacon J-003459-08) was used for siRNA studies. Polyplexes and solid NPs were prepared as described above, and the nucleic acid loading of solid NPs was measured using the PicoGreen or RiboGreen assays to determine the appropriate treatment amount per mg of particles. For both pDNA and mRNA studies, a total of 1 μg of pDNA or mRNA was used to treat a single well for all treatment conditions. As a control, Lipofectamine 2000 and Lipofectamine 3000 or TransIT reagents were used to deliver the same amount of pDNA or mRNA, respectively, according to manufacturer protocols. Cells were treated with pDNA for a total of 48−72 h and mRNA for a total of 24−48 h. EGFP expression was then quantified using flow cytometry. Transfection efficiency was determined as the percentage of cells expressing EGFP above expression levels of untreated control samples.

For siRNA treatment, a total of 5 pmol of siRNA (~0.1 μg) was used to treat a single well for all treatment conditions. As a control, Lipofectamine RNAiMAX was used to deliver the same amount of siRNA. Cells were treated with siRNA for a total of 48 h and subsequently harvested for either RNA extraction or protein extraction. Total RNA was isolated using the Qiagen RNeasy Mini Kit (Qiagen Inc., Hilden, Germany). Isolated RNA was used to

DOI: 10.1021/acs.biomac.8b00997
Biomacromolecules 2018, 19, 3861−3873

synthesize cDNA using a High Capacity cDNA Reverse Transcription Kit (Thermo Fisher Scientific). Transcript levels were measured by quantitative real-time PCR using an Applied Biosystems StepOnePlus Real-Time PCR System instrument using the TaqMan Fast Universal PCR Master Mix (Thermo Fisher Scientific). TaqMan primers for BIRC5 (Hs04194392_s1) and 18S rRNA (Hs99999901_s1) were used for gene expression analysis. All transcript levels were normalized to that of 18S rRNA in the same sample.

For immunoblotting analysis, cells were lysed with AZ lysis buffer supplemented with protease inhibitors (Roche, Basel, Switzerland), and protein concentrations were measured using the DC Protein Assay (Bio-Rad Laboratories, Hercules, CA, USA). Samples were then mixed with Laemmli sample buffer, boiled at 95 °C for 5 min, resolved by SDS-PAGE, and transferred to nitrocellulose membranes, which were blocked in 5% milk in Tris-buffered saline with Tween 20 (TBST) buffer. Blocked membranes were incubated overnight at 4 °C in blocking buffer containing antibodies specific for BIRC5 (71G4B7, Cell Signaling). An antibody specific for GAPDH (14C10, Cell Signaling) was used as a loading control. Signals were visualized using the SuperSignal West Pico PLUS Chemiluminescent Substrate kit (Thermo Scientific) on a BioRad ChemiDoc XRS+ imaging system.

Statistical Analysis. Results were analyzed using GraphPad Prism (GraphPad Prism version 7.04 for Windows, GraphPad Software, La Jolla, CA, USA, www.graphpad.com). The Student *t*-test or one-way ANOVA with Bonferroni's post-test were used where appropriate. Mean values represent at least three independent experiments and error bars represent the mean ± standard deviation or standard error of the mean as noted. For all statistical tests, $p < 0.05$ was considered statistically significant.

RESULTS AND DISCUSSION

Polymer Chemical, Thermal, and Surface Characterization. Three variants of the PACE polymer PPMS were synthesized (Figure 1); "PPMS" which is composed from monomers PDL, MDEA, and DES, "PPMS-COOH" composed of PDL, MDEA, SA, and "PPMS-PEG" composed of PDL, MDEA, DES, and PEG.

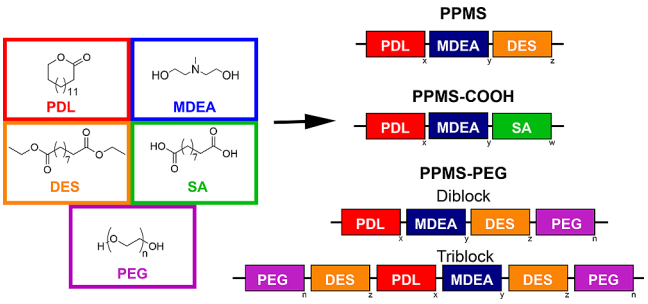

Figure 1. Synthesis of PPMS Polymers. Representation of monomer compositions for PPMS, PPMS-COOH, and the diblock and triblock PPMS-PEG.

For the remainder of this work, we define a nomenclature: the number after the dash indicates the molar percentage of PDL in the polymer (i.e., PPMS-30 refers to PPMS with 30% PDL content and PPMS-50PEG refers to PPMS-PEG with 50% PDL content). The substitution of SA for DES results in the formation of a carboxylic acid terminus on one end of the polymer chain. The addition of PEG into the synthesis produces two species: diblock (PPMS-PEG) and triblock (PEG-PPMS-PEG) as described prior.[24] Similar structures are formed when PEG is added to the COOH synthesis, and thus were not further investigated. Depending on the molar percentage of PDL used in the starting reactants, the polymer products varied from a clear viscous liquid (≤20% PDL) to a waxy semi-solid (30−40% PDL) to a white powder (≥50% PDL) at room temperature (Figure S1).

Polymer chemical structures were determined, and the monomer content was quantified using 1H-HMR. Although the synthesis protocol was modified from prior publications, the signature peaks described earlier were observed for synthesized PACE polymers and quantification was carried out using the same methods.[5,25] Spectra overlays at each increment of PDL molar content were determined for PPMS (Figure S2), PPMS-COOH (Figure S3), and PPMS-PEG (Figure S4). Monomer ratios and nitrogen content (and PEG content if applicable) were quantified (see Tables 1 and 2).

Table 1. Summary of Synthesis and Chemical Properties of PPMS and COOH PPMS

	molar ratio				
polymer	feed	^{1}H NMR	M_w (Da)	PDI	nitrogen content (%)
		PDL:DES:MDEA			
PPMS-10	10:45:45	16:38:46	24 700	2.11	4.52
PPMS-20	20:40:40	20:36:44	22 000	2.33	4.22
PPMS-30	30:35:35	30:26:44	23 100	1.78	3.09
PPMS-40	40:20:20	39:18:43	26 000	1.95	2.07
PPMS-50	50:25:25	57:13:30	54 500	2.22	1.50
PPMS-60	60:20:20	56:11:33	54 800	2.56	1.24
PPMS-70	70:15:15	69:3:28	62 500	2.25	0.40
PPMS-80	80:10:10	78:3:19	66 300	2.07	0.34
PPMS-90	90:5:5	88:2:10	75 000	2.13	0.28
		PDL:SA:MDEA			
PPMS-10COOH	10:45:45	10:41:49	17 500	1.93	4.88
PPMS-20COOH	20:40:40	22:30:48	15 000	1.43	3.58
PPMS-30COOH	30:35:35	34:34:32	28 500	2.27	4.03
PPMS-40COOH	40:20:20	42:34:24	28 000	2.25	4.06
PPMS-50COOH	50:25:25	51:19:30	69 100	2.25	2.26
PPMS-60COOH	60:20:20	60:18:22	73 600	2.30	2.17
PPMS-70COOH	70:15:15	69:11:20	77 300	2.40	1.28
PPMS-80COOH	80:10:10	79:6:15	82 100	2.35	0.71
PPMS-90COOH	90:5:5	90:6:4	92 200	2.35	0.66

In general, the composition of the polymer product reflects the reactant monomer input. Nearly all PDL content measurements are within 5% of the percentage expected based on monomer input ratios, with a few not unexpected outliers in the extremes (10% and 90%). Unlike prior reports of PACE syntheses, we observed a strong preferential addition of the diester over the amino-substituted diol despite their equivalent molar ratios in the synthesis reactants. This preference is particularly strong in polymers synthesized with 50% PDL or greater. The thermal properties of MDEA indicate that more energy is required to promote polymerization compared to DES or SA. Thus, DES and SA are more readily added to the polymer chain in this lower temperature enzyme-driven reaction environment compared to MDEA.

DOI: 10.1021/acs.biomac.8b00997
Biomacromolecules 2018, 19, 3861−3873

Table 2. Summary of Synthesis and Chemical Properties of PEG PPMS

	PDL:DES:MDEA molar ratio					
polymer	feed	^{1}H NMR	M_w (Da)	PDI	nitrogen content (%)	PEG content[a] (wt%)
PPMS-10PEG	10:45:45	16:38:46	15000	1.84	4.52	34.4
PPMS-20PEG	20:40:40	22:37:41	8500	2.08	4.36	33.9
PPMS-30PEG	30:35:35	30:36:34	11300	2.07	4.27	35.8
PPMS-40PEG	40:20:20	38:23:39	18400	2.24	2.69	35.2
PPMS-50PEG	50:25:25	49:17:34	21500	1.83	1.95	35.8
PPMS-60PEG	60:20:20	56:11:33	30900	1.93	1.25	33.7
PPMS-70PEG	70:15:15	69:8:23	39500	1.63	0.97	33.9
PPMS-80PEG	80:10:10	77:5:18	47100	2.10	0.55	36.3
PPMS-90PEG	90:5:5	85:2:13	49600	2.03	0.21	34.9

[a]All PPMS-PEG were synthesized with 32.5 wt% PEG in the starting reactants.

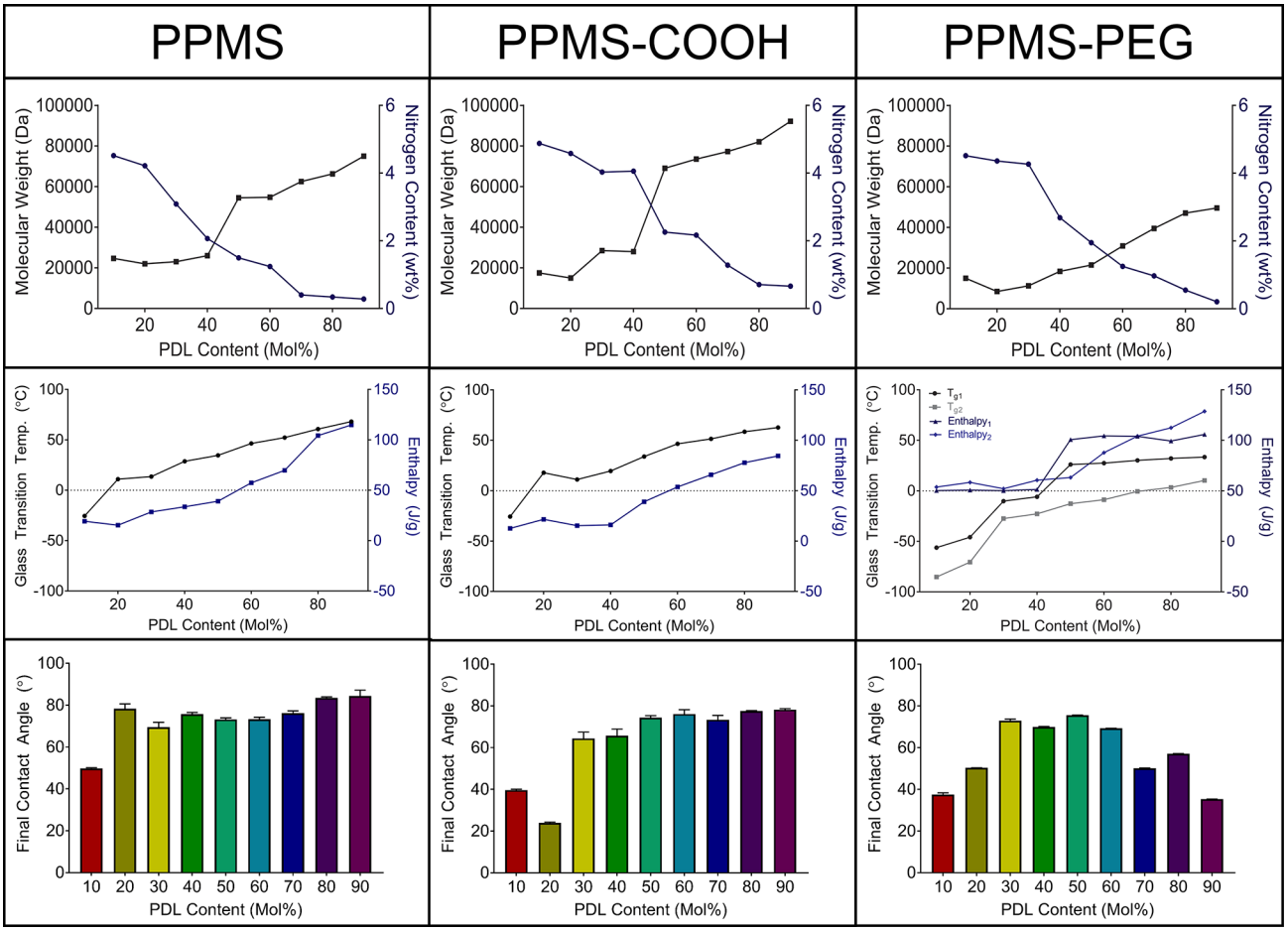

Figure 2. Physiochemical characterization of PPMS polymers. Top panels show the trends of molecular weight and nitrogen content in relation to PDL content. Middle panels illustrate the trends in thermal properties relative to PDL content. Bottom panels show the contact angle of water on polymer thin films in correlated to PDL content. Data are shown as mean ± standard deviation, n = 3 per group.

As expected, we observed a positive correlation between PDL content and molecular weight as well as a negative correlation with nitrogen content (Figure 2 top panels). It is also notable that the PDI values in these syntheses are equivalent or slightly lower than those reported in prior publications.[5,25−27] One key difference in this work is that we measured reactant ratios using molar ratios instead of weight percentages: it is possible that more control over the polymer synthesis output was achieved by this approach. There may also be significant differences in polymer molecular weights achieved due to the longer reaction times used in this method compared to prior methods. Unexpectedly, the highest molecular weights were achieved in PPMS-COOH, which were higher than PPMS, which were higher than PPMS-PEG. We anticipated that the carboxylic acid end group produced in PPMS-COOH would affect the synthesis. We expected the carboxylic acid end group to terminate polymer chain growth early thus leading to our hypothesis that PPMS would generate the highest molecular weight. Our results disprove our hypothesis demonstrating that the end group appears to promote chain length growth resulting in the highest molecular weights.

DOI: 10.1021/acs.biomac.8b00997
Biomacromolecules 2018, 19, 3861−3873

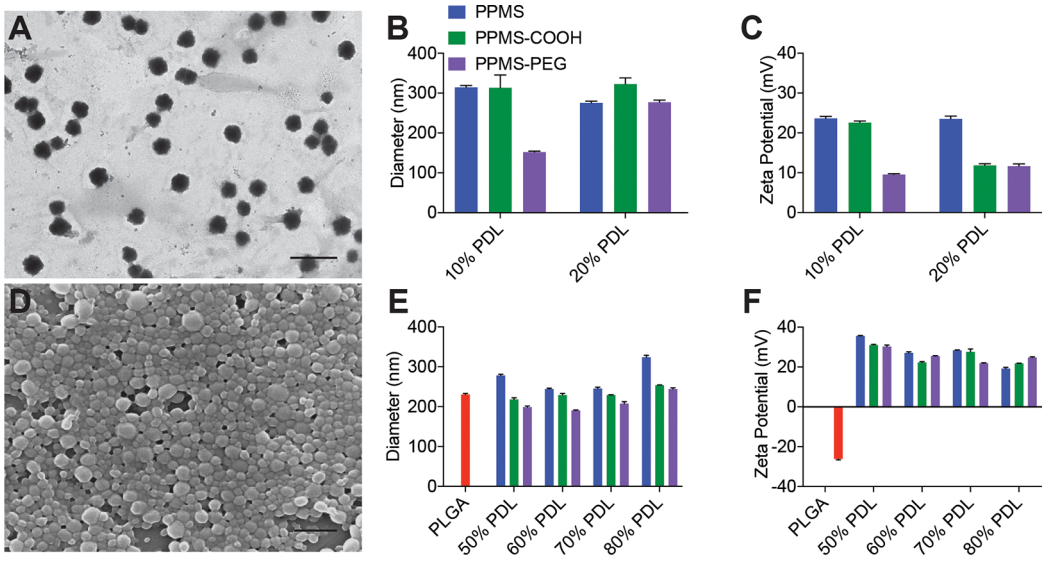

Figure 3. Characterization of PACE polyplexes and NPs. (A) A representative TEM image of polyplexes with spherical structure formulated with PPMS-10 complexed with short (19-bp) double stranded DNA with a 5′ Cy5 fluorescent tag at a 100:1 polymer:nucleic acid weight ratio. (B) Diameter (nm) and (C) zeta potential (mV) of polyplexes formulated with 10−20% PDL content PACE polymers. Mean ± standard error of the mean of three independent formulation batches is shown for size and zeta potential measurements. (D) A representative SEM image of spherical solid PPMS-60 NPs loaded with DiO. (E) Diameter (nm) and (F) zeta potential (mV) of DiO-loaded NPs formulated with 50−80% PDL content PACE polymers. Mean ± standard error of the mean of three independent formulation batches are shown for size and zeta potential measurements. Scale bars, 1 μm.

In this case, it appears the addition of a functional end group, such as a carboxylic acid, promoted further chain growth rather than prohibiting it. The polymerization of PACE polymers follows a typical polycondensation step-growth mechanism. During the condensation reactions, small molecules such as water and alcohols are eliminated during the step-growth.[28] The condensation reaction of the carboxylic acid end group predominately produces water while other end group chemistries likely produce ethanol in combination with water. The production of ethanol requires more energy than the production of water, therefore, the step-growth of carboxylic acid end group polymers can occur at a faster rate than the other end group chemistries. As all of these reactions were performed using the same time line, the faster rate of polymerization of the carboxylic acid polymers resulted in the highest molecular weights. Therefore, carboxylic acid end groups lead to higher chain growth than the other end group chemistries. Consistent in each PACE variety, the lowest molecular weight was achieved at 20% PDL. At this time, it is unclear why 20% PDL would generate a shorter polymer chain compared to 10% PDL; however, polymer performance is significantly impacted by this feature, as we describe later.

Similar positive correlation was observed between PDL content and thermal properties (Figure 2 middle panels). As PDL content increased, both the glass transition temperature (T_g) and enthalpy increased. The increase in PDL content decreases chain mobility due to its large size, which further increases the amount of energy required to break intermolecular bonds. The mild broadness observed in the T_g peaks on the DSC is likely due to a gradient polymer build (Figures S5−S7). Essentially, during synthesis with overabundance of one monomer, in this case PDL, multiple PDL monomers are likely added early in chain growth with the other monomers interspersed. Polymers with monomer gradients—such as styrene/4-hydroxystyrene or poly(styrene-*co*-methyl methacrylate)—tend to exhibit broad transitions unlike homopolymers (such as polycaprolactone (PCL) or Poly(lactic acid) (PLA)) that have sharp transitions.[29−31] The energy required for this endothermic process is large and easily visualized via DSC, as we observed here (Figures S5−S7).

In prior work, it has been described that two varieties are synthesized when PEG is incorporated into a traditional PPMS synthesis: diblock and triblock.[24,32] Despite the significantly different structures produced in diblock and triblock, the added molecular weight of 5K PEG is not enough to produce distinguishable retention times in traditional GPC; thus, diblock and triblock species cannot be easily separated. But two peaks were observed in the PPMS-PEG heat flux curves on DSC, which are the result of differences in T_g and enthalpy values between diblock and triblock (Figure S7). Although there is no possibility of using DSC to separate these two species of PPMS−PEG, future studies could investigate the relative percentages of diblock and triblock formed via DSC. This might lead to the development of synthesis methods that control species formation.

Surface properties of solvent casted films were examined using the sessile drop method (Figure 2 bottom panels). As expected, there were discernible differences in surface properties based on differences in composition. Both PPMS and PPM-COOH have similar linear positive correlations; an increase in contact angle was observed with increased PDL content. This indicates increased hydrophobicity on the surface of the film with increasing PDL content, which is expected due to the hydrophobic PDL unit. Many degradable polyesters that are commonly used as biomaterials, such as PLA and Poly(lactic-co-glycolic acid) (PLGA), also exhibit high contact angles (~70°)[33] and often hydrophobicity can be modified using techniques from micropatterning to surface chemistry modification.[34−36] One such technique is to PEGylate the surface in order to increase hydrophilicity. Here, PEG was incorporated directly into PPMS in the starting reactants instead of using a post-processing technique. The

DOI: 10.1021/acs.biomac.8b00997
Biomacromolecules 2018, 19, 3861−3873

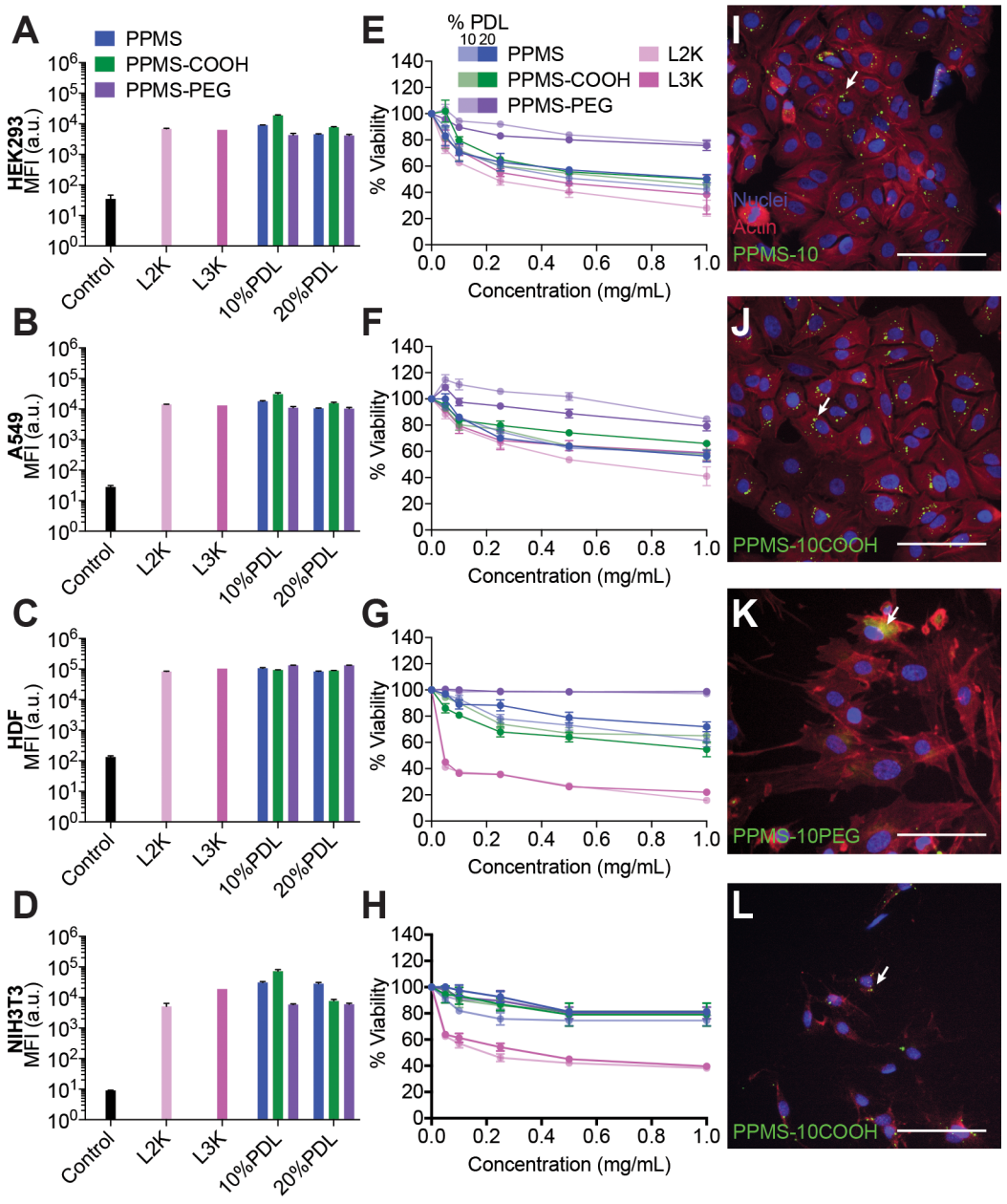

Figure 4. PACE polyplex uptake and biocompatibility. (A–D) Uptake (mean fluorescence intensity (MFI)) of PACE polyplexes or Lipofectamine 2000 and 3000 encapsulating a fluorescently labeled short dsDNA in HEK293, A549, HDF, and NIH3T3 cell lines, respectively, as measured by flow cytometry. Mean ± standard error of the mean of three independent replicates are shown. (E–H) Biocompatibility/cell viability of HEK293, A549, HDF, and NIH3T3 cell lines, respectively, following treatment with various concentrations of PACE polyplexes and equivalent doses of Lipofectamine 2000 and 3000 for 24 h as measured by the neutral red viability assay. Mean ± standard error of the mean of three independent replicates is shown for each concentration. (I–L) Fluorescence images of HEK293, A549, HDF, and NIH3T3 cell lines, respectively, treated with the indicated polyplexes encapsulating fluorescent dsDNA. Nuclei are shown in blue, and actin is shown in red. Arrows indicate perinuclear localization of polyplexes. Scale bars, 50 μm.

addition of PEG significantly altered the observed contact angle. From 10 to 50% PDL content an increase in contact angle is observed, similar to that of PPMS and PPMS-COOH; however, a decrease in contact angle was observed as PDL content increased from 60 to 90% PDL. This observation may be an artifact of our experimental approach, in which solvent casting was used to create films on a glass slide; the seemingly more hydrophilic surface at higher PDL content may be due to PEG orienting itself away from the hydrophobic glass and toward the air interface. For all PDL contents, contact angles were significantly lower for PPMS-PEG compared to the respective counterparts. This decrease in contact angle is desirable for producing medical devices such as scaffolds, where more hydrophilic surfaces can resist protein adsorption or cell adhesion. This may be a disadvantage for gene delivery vectors, as nanomaterials that are more resistant to cell adhesion may also be more resistant to cell entry.

PACE Delivery Vehicle Characterization. PACE polymers were formulated into two alternate delivery vehicles depending on PDL content. Polymers with a 10–20% molar PDL content that are viscous liquids at room temperature were formulated into polyplexes with short (19-bp) double stranded

DOI: 10.1021/acs.biomac.8b00997
Biomacromolecules 2018, 19, 3861–3873

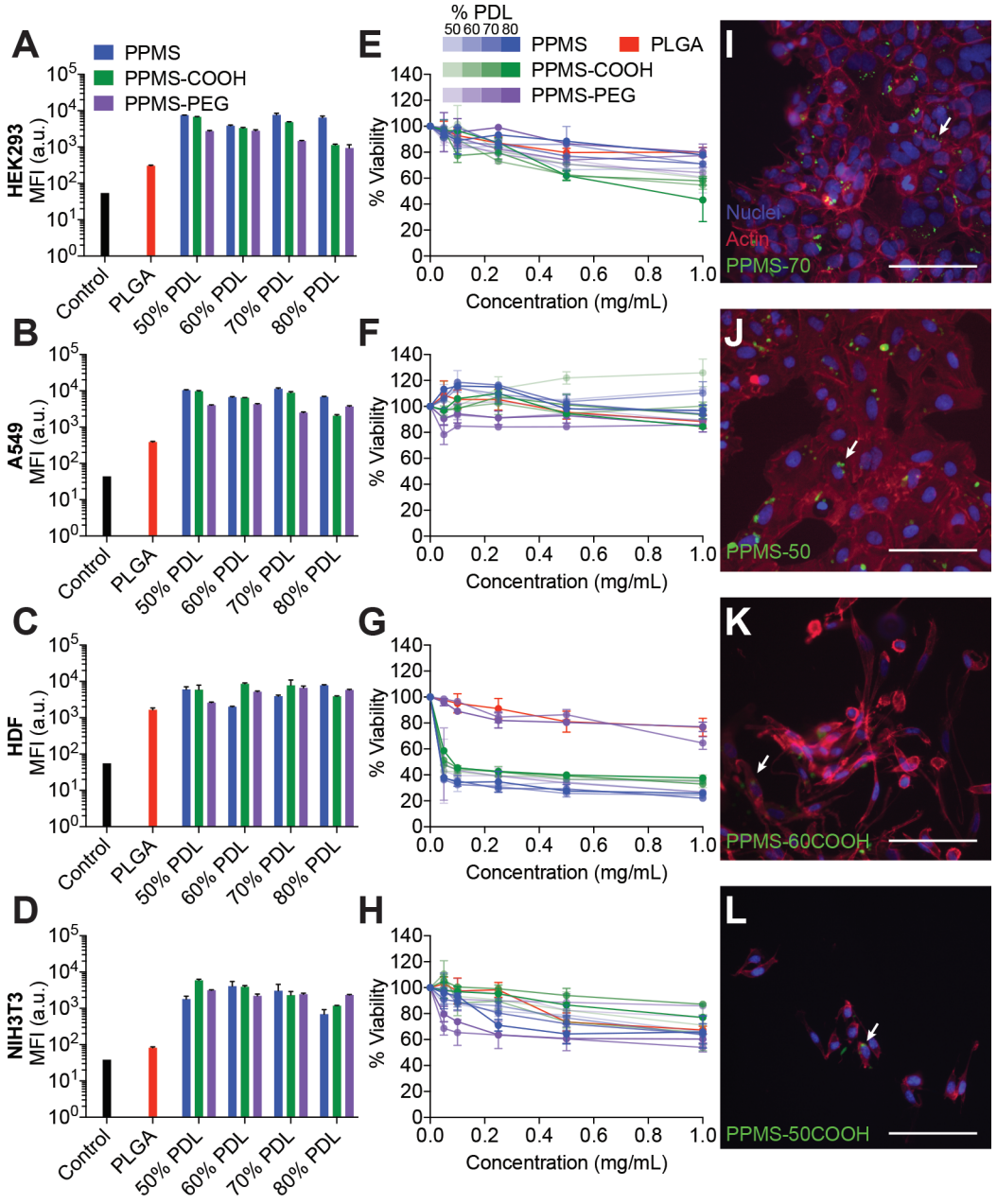

Figure 5. Solid PACE NP uptake and biocompatibility. (A–D) Uptake (mean fluorescence intensity (MFI)) of DiO-loaded PACE or PLGA NPs in HEK293, A549, HDF, and NIH3T3 cell lines, respectively, as measured by flow cytometry. Mean ± standard error of the mean of three independent replicates are shown. (E–H) Biocompatibility/cell viability of HEK293, A549, HDF, and NIH3T3 cell lines, respectively, following treatment with various concentrations of PACE and PLGA NPs for 24 h as measured by the neutral red viability assay. Mean ± standard error of the mean of three independent replicates is shown for each concentration. (I–L) Fluorescence images of HEK293, A549, HDF, and NIH3T3 cell lines, respectively, treated with the indicated DiO-loaded PACE NPs. Nuclei are shown in blue, and actin is shown in red. Arrows indicate perinuclear localization of polyplexes. Scale bars, 50 μm.

fluorescently tagged DNA. Polymers with a 50–80% PDL content that are in a more solid state at room temperature were formulated into solid NPs loaded with a fluorescent dye (DiO) using a single emulsion solvent evaporation technique. For low PDL contents, PPMS and PPMS-COOH produced polyplexes ~300 nm in size as expected due to the similarities in their molecular weights (Figure 3A,B). PPMS-10PEG polyplexes were smaller in size, with a diameter of 150 nm, whereas PPMS-20PEG polyplexes were similar in size to PPMS and PPMS-COOH polyplexes. As expected, the diameters of PPMS-PEG polyplexes are stable over time, whereas the larger unPEGylated polyplexes are more variable (Figure S8). While polyplexes are intended for immediate use, these results suggest that formulations incorporating PEGylated polymers could be used for nucleic acid delivery over longer periods if desired. All polyplexes had a positive surface charge (Figure 3C). PPMS and PPMS-COOH exhibited similar positive surface charges (~23 mV) except for PPMS-20COOH. Both PPMS and PPMS-10COOH formulations had molecular weights greater than 17.5 kDa and nitrogen contents ranging from 4.2 to 4.9%. Polyplexes formed from PPMS-20COOH and PPMS-PEG had mildly positive surface charges (9–11 mV), likely due to their similar

DOI: 10.1021/acs.biomac.8b00997
Biomacromolecules 2018, 19, 3861–3873

molecular weights that are less than or equal to 15 kDa and nitrogen contents ranging from 3.5 to 4.5%.

For high PDL contents, the solid NP formulation yielded similar trends in size as found in the polyplex formulations. PPMS and PPMS-COOH NPs had comparable size ranges, while formulations of PPMS-PEG were notably smaller (Figure 3D,E). PPMS-COOH exhibited a narrower size distribution (220−250 nm) compared to PPMS (190−320 nm). The discernible difference in size distribution could be attributed to polymer nitrogen content and molecular weight. PPMS polymers had lower nitrogen contents and lower molecular weights from 50 to 90% compared to their respective PPMS-COOH counterparts, which could explain these differences in size and dispersity. Nonetheless, all formulation size distributions were similar to what has been previously reported for siRNA-loaded solid PPMS NPs.[17] They were also similar in size to PLGA NPs (230 nm); PLGA is used for comparison because it is a solid at room temperature like the higher PDL content PACE polymers and it forms solid NPs when formulated using the same emulsion solvent evaporation formulation techniques. As expected, all PACE NPs exhibited a positive surface charge (Figure 3F). Higher magnitudes of positive surface charges were found with formulations from polymers with lower PDL content and thus higher nitrogen content. Generally, NPs formulated with 50% PDL polymers had surface charges ∼30 mV, while those with 80% PDL polymers were closer to 20 mV.

These characterization results suggest that PACE family polymers offer a high degree of customization that can be translated into delivery vehicle formulation. Varying the monomer combinations, particularly varying the PDL content, can lead to the fine-tuned repeatable production of delivery vehicles of a known size distribution and surface charge while using standard formulation techniques. Most importantly, the control of the mildly cationic surface charge can improve the loading of negatively charged materials (such as nucleic acids) and facilitate enhanced interactions with the cell membrane.[37]

PACE Polyplex and NP Uptake and Biocompatibility. Polyplex and solid NP PACE formulations of varying chemical compositions were tested for uptake and biocompatibility in four cell lines: human embryonic kidney (HEK293), human lung carcinoma (A549), human dermal fibroblast (HDF), and mouse embryonic fibroblasts (NIH 3T3) (Figures 4 and 5). Cellular uptake can either be mediated by specific receptors on the cell surface or non-specific. Nanocarriers with a cationic charge are generally attracted to negatively charged proteoglycans on the cell surface, promoting non-specific uptake.[37] As expected, cationic PACE polyplexes formulated using a fluorescently labeled short 19-bp dsDNA resulted in cellular uptake in all four cell lines, with fluorescence values 2−4 orders of magnitude higher than untreated control cell populations (Figure 4A−D). Further, uptake of all PACE polymers was comparable to or greater than commercially available Lipofectamine 2000 or 3000 reagents. Cell viability after exposure to polyplexes and an equivalent dose of Lipofectamine 2000 or 3000 was also measured (Figure 4E−H). Uptake of polyplexes and their perinuclear intracellular localization was confirmed using epifluorescence microscopy (Figure 4I−L). While all PACE polyplex formulations were taken up efficiently, certain polymer compositions were found to yield the highest uptake, which also varied with cell type. PPMS-10COOH polyplexes were most efficiently uptaken in HEK293, A549, and NIH 3T3 cells while PPMS-10PEG polyplexes were most readily internalized in HDFs. The preference for PPMS-10COOH might be explained by the fact that this polymer had the highest nitrogen content (4.88%). HDFs were the most sensitive to higher cationic charge (Figure 3G), thus the addition of the PEG monomer to generate a more hydrophilic and less cationic vehicle likely aided with polyplex internalization in this cell line.

Mild cytotoxicity was observed in all cell lines for PPMS and PPMS-COOH polyplex formulations when delivered at concentrations above 0.2 mg/mL (Figure 4E−H). There were no clear trends in cytotoxicity with PDL content. Negligible or minimal cytotoxicity was observed for all PPMS-PEG formulations, suggesting that these polyplexes are the most biocompatible. Cell viability was higher in PACE polyplex-treated cells than in cells treated with Lipofectamine 2000 or 3000 at an equivalent dose across the cell types tested; Lipofectamine 2000 exhibited the highest cytotoxicity. Importantly, typical polyplex treatment concentrations result in cell exposure to 0.1 mg/mL PPMS,[5,38] which appears to be well within the tolerable range across the cell types tested for all of the low PDL content PACE varieties tested. These formulations are also less toxic than Lipofectamine; we have previously reported increased cytotoxicity of Lipofectamine compared to PPMS with equivalent cargo treatment levels in A549 cells.[5]

Fluorescent DiO-loaded solid PACE NPs were also tested for uptake in the same cell lines (Figure 5). In this case, NPs were compared to DiO-loaded PLGA NPs that were prepared using the same emulsion methods. Similar to the trends observed with polyplexes, high uptake of solid NPs was detected across all polymer varieties (Figure 5A−D). Again, the cell lines tested exhibited at least 2−3 orders of magnitude higher fluorescence upon treatment with PACE NPs compared to untreated controls (Figure S9). Further, all NP varieties exhibited higher uptake compared to PLGA NPs, and in some cases the difference was substantial (over an order of magnitude increase in MFI). Viability after exposure to particles was measured (Figure 5E−G) and uptake results were confirmed with epifluorescence microscopy (Figure 5I−L). Again, while uptake levels were high for all formulations, cell type preferences were observed. For solid NPs, HEK293 and A549 cells exhibited the highest uptake with PPMS compositions across PDL contents while PPMS-COOH was most highly taken up in HDFs and NIH 3T3 cells, though there were several high-performing polymer compositions in the fibroblast cell lines. Nitrogen content, which was significantly lower for higher PDL content PACE polymers compared to lower PDL content polymers, does not appear to play as large a role in cell type preferences for PACE NPs as with PACE polyplexes in terms of uptake. Delivery vehicle size may in this case be more important. PPMS-COOH NPs are generally smaller in size compared to PPMS NPs (Figure 3), which may have facilitated uptake in the fibroblast cells with more mesenchymal morphology. While PPMS-PEG NPs are also small, the addition of PEG generally reduces nonspecific uptake.[39]

When unloaded (blank) solid NPs were tested for cell toxicity, they were well tolerated by most cell lines (Figure 5E−H). Minimal toxicity was observed for all polymer varieties in A549 cells (Figure 5F). The other three cell types exhibited varying tolerances for the different NP compositions. HEK293 cells tolerated all particle types at concentrations below 0.3 mg/mL (Figure 5E) with more noticeable toxicity observed

DOI: 10.1021/acs.biomac.8b00997
Biomacromolecules 2018, 19, 3861−3873

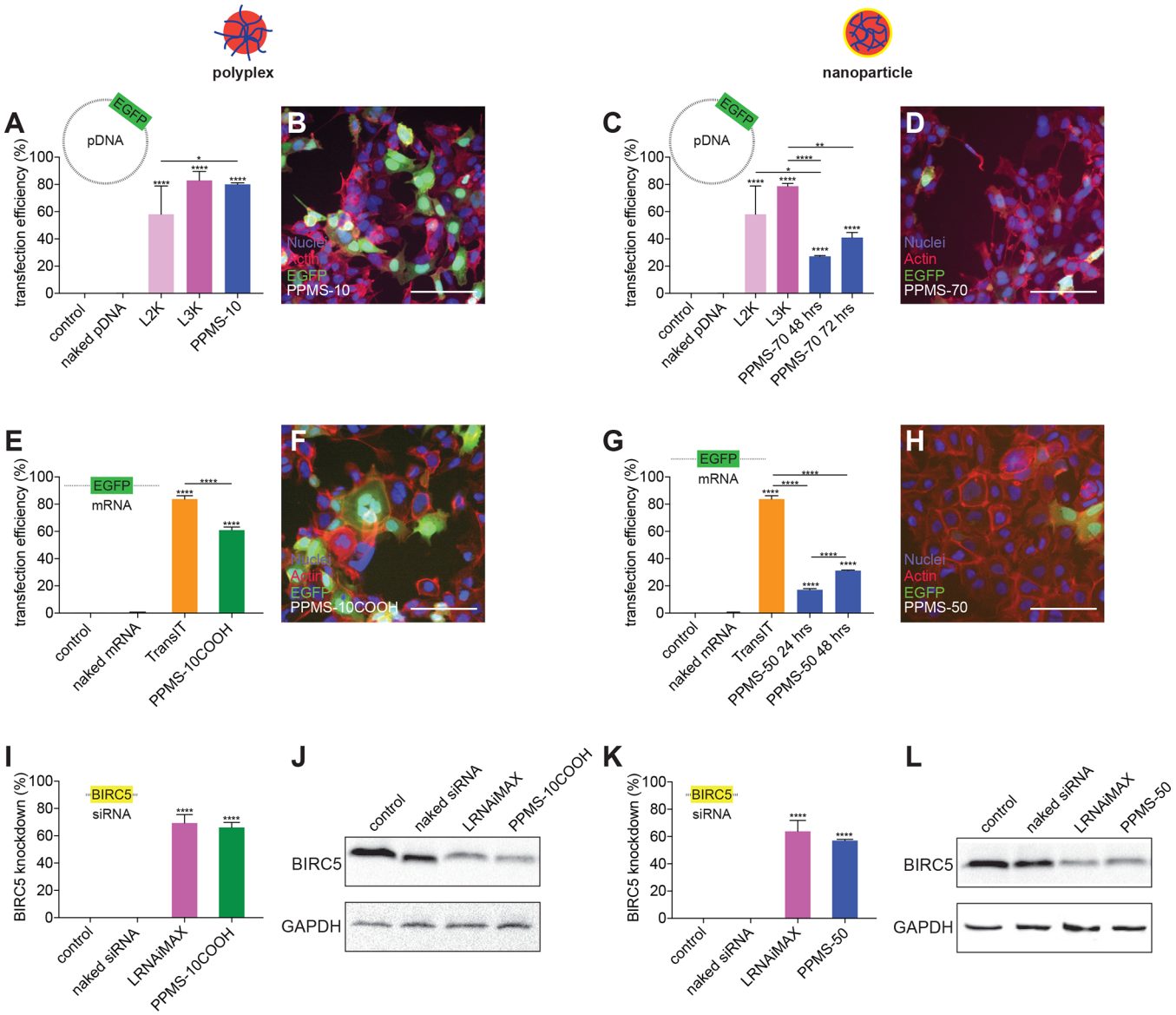

Figure 6. Transfection of pDNA, mRNA, and siRNA by PACE Polyplexes and NPs. Efficiency of EGFP plasmid delivery with (A) PPMS-10 polyplexes and (C) PPMS-70 NPs compared to Lipofectamine 2000 and 3000 quantified by flow cytometry. Mean ± standard error of the mean of three independent replicates is shown. Representative fluorescence images of EGFP expression following pDNA delivery by (B) PPMS-10 polyplexes and (D) PPMS-70 NPs. Nuclei are shown in blue and actin is shown in red. Efficiency of EGFP mRNA delivery with (E) PPMS-10COOH polyplexes and (G) PPMS-50 NPs compared to TransIT quantified by flow cytometry. Mean ± standard error of the mean of three independent replicates is shown. Representative fluorescence images of EGFP expression following mDNA delivery by (F) PPMS-10COOH polyplexes and (H) PPMS-50 NPs. Nuclei are shown in blue and actin is shown in red. Efficiency of siRNA delivery as measured by relative mRNA levels of Survivin (BIRC5) via RT-PCR with (I) PPMS-10COOH polyplexes and (K) PPMS-50 NPs compared to Lipofectamine RNAiMAX. Mean ± standard error of the mean of three independent replicates is shown. Efficiency of siRNA delivery as measured by immunoblot protein levels of BIRC5 with (J) PPMS-10COOH polyplexes and (L) PPMS-50 NPs compared to Lipofectamine RNAiMAX. *P < 0.05, **P < 0.01, ****P < 0.0001. Scale bars, 50 μm.

using PPMS-COOH polymers, which had the highest nitrogen contents. On the other hand, primary HDFs exhibited a decrease in viability when exposed to PPMS and PPMS-COOH at concentrations as low as 0.05−0.1 mg/mL (Figure 5G). In contrast, PPMS-PEG polymers were well-tolerated by this cell line even at high concentrations (up to 1 mg/mL). NIH 3T3 fibroblasts tolerated all PACE varieties, even at high concentrations. Lower PDL and higher amine content polymers generally resulted in decreased viability, especially in HEK293 and HDF cells, but cytotoxicity did not always correlate with PDL content across cell types and polymer chemistries. Although some toxicity was observed at higher NP concentrations, particularly in primary HDF cells as expected, typical treatment concentrations for PACE NPs are ∼0.1 mg/mL,[17] a concentration which was well tolerated by the majority of cell types tested. Moreover, NPs loaded with negatively charged nucleic acids will present reduced surface zeta potential, as has been observed previously,[17] leading to a milder cationic charge which is likely to result in less cytotoxicity.

Together, the uptake and viability results for polyplexes and PACENPs indicate that cellular toxicity and association vary

DOI: 10.1021/acs.biomac.8b00997
Biomacromolecules 2018, 19, 3861−3873

with the chemical composition of the delivery vehicles as well as cell type. This variability in cellular responses highlights the benefits of a versatile family of polymers with easily tunable chemical and physical properties. Having such a library allows for one to choose optimal delivery vehicles (i.e., those that are balanced in terms of high transfection efficiency and acceptable biocompatibility) for a target cell type of interest. As multiple factors are involved in the delivery of nucleic acid therapeutics to cells, after determining the best PACE polymer types in terms of cell association and toxicity, further screens based on the type of nucleic acid cargo to be delivered and any desirable formulation characteristics (ex. size) can be used to finalize the choice of delivery vehicle. In the following section, we illustrate these principles for the delivery of pDNA, mRNA, and siRNA.

Effective Delivery of Nucleic Acids Using PACE Formulations. Promising polymer compositions were further tested for their ability to deliver a range of nucleic acids to HEK293 cells. Specifically, the delivery of pDNA, mRNA, and siRNA using polyplexes or NPs was compared to the delivery of the same nucleic acids by commercially available agents (Figure 6). For HEK293 cells, we elected to test polyplexes of PPMS-10 for delivery of pDNA because these polyplexes were efficiently taken up in this cell line, and PPMS-10 is similar to PACE family polymers that have been previously used to deliver pDNA successfully.[5] PPMS-10 polyplexes encapsulating pDNA encoding EGFP resulted in a transfection efficiency of ∼80% after 48 h as determined using flow cytometry to quantify the percentage of cells expressing EGFP. Transfection with PPMS-10 was significantly higher than Lipofectamine 2000 (58%) and comparable to Lipofectamine 3000 (82%) (Figure 6A). Transfection of the EGFP plasmid was confirmed using epifluorescence microscopy (Figure 6B). HEK293 cells were also treated with PPMS-70 solid NPs encapsulating EGFP pDNA at equivalent payload concentrations. This polymer was chosen due to its high uptake in HEK293 cells (Figure 5A). In this case, despite high nucleic acid loading (∼78% encapsulation efficiency), transfection efficiency was lower than the polyplex-treated cells after a standard treatment of 48 h (27%) (Figure 6C,D and Table S1). However, an increase in transfection efficiency was noted 72 h after treatment (41%), which was consistent with slow pDNA release from these particles (Figure S10). This is an important benefit for *in vivo* administration, as polyplexes are generally not capable of sustained release. EGFP expression after transfection with commercial reagents such as Lipofectamine 2000 is decreased after 72 h compared to 24 h and 48 h.[40] Importantly, pDNA-loaded PPMS-70 NPs were also larger (∼400 nm) than the DiO-loaded PPMS-70 NPs used in the uptake studies, which could also affect transfection efficiency (Figure 3 and Table S1).

Similar experiments were performed to test the efficiency of PACE polymers to deliver mRNA encoding EGFP. We chose to examine the delivery potential of PPMS-10COOH because similar polymer chemistries have been successful for mRNA delivery.[18] Here, administration of PPMS-10COOH polyplexes resulted in a transfection efficiency of 61% compared to 83% achieved using TransIT Transfection Reagent (Mirus Bio) (Figure 6E). Transfection of EGFP mRNA was once again confirmed by microscopy (Figure 6F). While mRNA transfection with PPMS-10COOH polyplexes was lower than that of TransIT, the transfection efficiency of PACE polymers can be increased by chemically modifying the polymers post-synthesis to improve cell association. We have recently reported that modifying end-group chemistry using "top-down" alterations to the PPMS or PPMS-COOH polymer result in significantly increased *in vitro* mRNA transfection efficiency, yielding efficiencies comparable to TransIT.[18] The ability to further modify PACE family polymers post-synthesis adds to the customizability of this platform. The transfection efficiency of solid PPMS-50 NPs that exhibit high uptake (Figure 3) and effectively encapsulate EGFP mRNA (∼91% encapsulation efficiency, Table S1) was also studied. Similar to pDNA delivery by solid PPMS-50 NPs, transfection efficiency was lower than that of PPMS-10COOH polyplexes after the standard treatment time of 24 h (17%) but increased after 48 h (31%) (Figure 6G,H), once again suggesting that sustained release of nucleic acid cargo is possible with solid NPs (Figure S10) that is not achievable with polyplexes or commercial agents. As with pDNA-loaded PPMS NPs, the size of mRNA-loaded PPMS-50 particles was also larger than DiO-loaded NPs at ∼320 nm (Figure 3 and Table S1). Importantly, pDNA (∼6000 bp) and mRNA (∼1000 bases) are larger nucleic acids compared to shorter siRNA and miRNA molecules (∼20 bases or bp), which affects delivery vehicle size as well as release from compact solid NPs (Figure S10) compared to more loosely complexed polyplexes that readily release nucleic acid cargo of any size. Nonetheless, this slower release of cargo, which is likely governed both by NP degradation and by decomplexation of negatively charged nucleic acid cargo and cationic polymer, could be used as an advantage in treatment modalities for which extended exposure to nucleic acids is beneficial.[17]

PACE polymers were also evaluated for their ability to deliver siRNA against Survivin (BIRC5), which has been previously delivered in NPs as a potential therapy for bladder cancer.[41] Knockdown of the BIRC5 gene was measured at both the mRNA level by quantitative real-time PCR (qRT-PCR) and at the protein level by immunoblot. In this case, knockdown efficiency by PACE polymers was compared to knockdown by Lipofectamine RNAiMAX. Given our success using PPMS-10COOH for RNA delivery of mRNA,[18] we chose to test the ability of this formulation to deliver siRNA. Treatment with PPMS-10COOH polyplexes encapsulating BIRC5 siRNA resulted in 67% knockdown of BIRC5 mRNA on average, which was comparable to the 69% knockdown efficiency observed using Lipofectamine RNAiMAX (Figure 6I). Knockdown was confirmed by Western blot analysis, and there was no discernible difference between samples treated with PPMS-10COOH or Lipofectamine—both exhibit clear knockdown compared to untreated samples and those treated with naked siRNA (Figure 6J). We further tested the ability of solid PPMS-50 NPs to deliver siRNA, as we have been successful with similar formulations.[17] In this case BIRC5 mRNA knockdown following treatment by PPMS-50 NPs encapsulating BIRC5 siRNA (∼85% encapsulation efficiency) was not significantly different than Lipofectamine RNAiMAX after 48 h of treatment with a knockdown efficiency of 57%, achieving similar knockdown to PPMS-10COOH siRNA polyplexes (Figure 6K). Knockdown of BIRC5 by PPMS-50 NPs was also confirmed at the protein level by immunoblot (Figure 6L). In this case, solid PACE NPs encapsulating the 19-bp siRNA achieve high knockdown within the standard 48 h treatment window typically used for Lipofectamine and PPMS polyplexes, likely due to faster nucleic acid release (Figure S10). Moreover, the size of siRNA-loaded PPMS-50 (∼250 nm) was similar to the DiO-loaded NPs studied (Figure

DOI: 10.1021/acs.biomac.8b00997
Biomacromolecules 2018, 19, 3861−3873

3 and Table S1) which exhibited high uptake (Figure 5). On the whole, as expected, the PACE polymer formulations that performed well in the uptake studies with HEK293 cells also achieved high nucleic acid loading and significant transfection levels in the same cell line, though the degree of success depended on the type of nucleic acid. Together, these results suggest that PACE polyplexes and NPs can serve as reliable nucleic acid delivery agents for a variety of cell types, but that the efficiency and timing of transfection will vary with the cell type of interest as well as the properties of the nucleic acid cargo being encapsulated.

CONCLUSIONS

The highly customizable family of PACE polymers has great potential for use as therapeutic tools and biomedical devices, offering a platform to deliver a variety of nucleic acids to different target cell types both *in vitro* and *in vivo*. The flexibility of synthesis yields a family of polymers with distinct characteristics that can be formulated into both polyplexes and solid NPs. Polyplexes and NPs formulated with PACE polymers formed mildly cationic nanosized vehicles that were readily internalized by a variety of different cell types, highlighting the strong cell association potential of PACE polymers. Further, PACE polymers were well tolerated by cells within a reasonable therapeutic treatment concentration range. PACE vehicles were also effective at nucleic acid delivery, mediating the transfection of pDNA, mRNA, and siRNA into HEK293 cells. Polyplex PACE formulations exhibited transfection efficiencies comparable to commercial transfection agents, with the added benefits of being adaptable, biocompatible, and biodegradable compared to their more cytotoxic commercial counterparts, which are also not readily biodegradable. PACE NP formulations had an additional advantage of extended release of nucleic acid cargo, particularly for larger pDNA and mRNA cargo, which could be an important attribute for *in vivo* applications.

Importantly, choosing an optimal delivery vehicle depends on the cell type of interest as well as the nucleic acid cargo. Indeed, multiple parameters are involved in orchestrating cellular internalization of vehicles and optimizing their cargo release. These processes will naturally be influenced by both the physicochemical properties of the delivery vehicles themselves as well as the specific nucleic acid payload. We have shown here that small differences in the structure and properties of polymeric materials for gene delivery can result in substantial changes in transfection efficiency. The advantage of the library of polymers shown here is that simple alteration of polymer chemical composition can easily overcome cell type preferences and limitations. Moreover, favorable delivery vehicle characteristics might further guide polymer synthesis. In short, the PACE delivery platform may alleviate some of the challenges associated with delivery to hard-to-transfect primary and stem cells, with potential applications both *in vitro* and *in vivo*. Further, this polymer family introduces new mildly cationic polymers into the arena of biodegradable medical devices with the added feature of nucleic acid delivery.

ASSOCIATED CONTENT

Supporting Information

The Supporting Information is available free of charge on the ACS Publications website at DOI: 10.1021/acs.biomac.8b00997.

Physical appearance of synthesized PACE family polymers; ^{1}H NMR spectra of PPMS, PPMS-COOH, and PPMS-PEG formulations; DSC curves of PPMS, PPMS-COOH, and PPMS-PEG formulations; stability of polyplexes; FACS and microscopy studies of uptakes of PLGA and optimal performing PACE NPs; and nucleic acid loading and release from optimal performing PACE NPs, including Figures S1−S10 and Table S1 (PDF)

AUTHOR INFORMATION

Corresponding Author

*W.M.S.: Malone Engineering Center 413, 55 Prospect St., New Haven, CT 06511. Phone: (203) 432-3281. Fax: (203) 432-0030. E-mail: mark.saltzman@yale.edu.

ORCID

W. Mark Saltzman: 0000-0002-2163-549X

Author Contributions

$^{\perp}$A.C.K. and A.S.P.-D. contributed equally to this work.

Notes

The authors declare no competing financial interest.

ACKNOWLEDGMENTS

We thank Zhenting Jiang for assistance with SEM, Michael Rooks for assistance with TEM, and Tushar Agarwal for assistance with Figure S8. This work was supported in part by a grant from the National Institutes of Health (NIH, R01HL125892). A.C.K. was supported by a NIH NRSA T32 (T32DK101019) Postdoctoral Fellowship. A.S.P. was supported in part by NIH NRSA T32 (T32GM86287) and F32 (F32HL142144) Postdoctoral Fellowships.

ABBREVIATIONS

BCS, bovine calf serum; CALB, *Candida antarctica* lipase B; DES, diethyl sebacate; DMEM, Dulbecco's modified Eagle's medium; DSC, differential scanning calorimetry; GPC, gel permeation chromatography; HDF, human dermal fibroblast; HEK293, human embryonic kidney 293; MALS, multiangle light scattering; MDEA, *N*-methyldiethanolamine; MFI, mean fluorescence intensity; NP, nanoparticle; ^{1}H NMR, proton nuclear magnetic resonance; PACE, poly(amine-*co*-ester); PEG, polyethylene glycol; PDL, 15-pentadecanolide; PPMS, poly(pentadecalactone-*co*-*N*-methyldiethanolamine-*co*-sebacate); SA, sebacic acid; SEM, scanning electron microscopy; TEM, transmission electron microscopy

REFERENCES

(1) Stewart, M. P.; Sharei, A.; Ding, X.; Sahay, G.; Langer, R.; Jensen, K. F. In vitro and ex vivo strategies for intracellular delivery. *Nature* **2016**, *538*, 183−192.

(2) Bouard, D.; Alazard-Dany, N.; Cosset, F. L. Viral vectors: from virology to transgene expression. *Br. J. Pharmacol.* **2009**, *157*, 153−165.

(3) Zhu, L.; Mahato, R. I. Lipid and polymeric carrier-mediated nucleic acid delivery. *Expert Opin. Drug Delivery* **2010**, *7*, 1209−1226.

(4) Juliano, R. L. The delivery of therapeutic oligonucleotides. *Nucleic Acids Res.* **2016**, *44*, 6518−6548.

(5) Zhou, J.; Liu, J.; Cheng, C. J.; Patel, T. R.; Weller, C. E.; Piepmeier, J. M.; Jiang, Z.; Saltzman, W. M. Biodegradable poly(amine-co-ester) terpolymers for targeted gene delivery. *Nat. Mater.* **2012**, *11*, 82−90.

(6) Kostritskii, A. Y.; Kondinskaia, D. A.; Nesterenko, A. M.; Gurtovenko, A. A. Adsorption of Synthetic Cationic Polymers on

DOI: 10.1021/acs.biomac.8b00997
Biomacromolecules 2018, 19, 3861−3873

Model Phospholipid Membranes: Insight from Atomic-Scale Molecular Dynamics Simulations. *Langmuir* **2016**, *32*, 10402−10414.
(7) Bishop, C. J.; Kozielski, K. L.; Green, J. J. Exploring the role of polymer structure on intracellular nucleic acid delivery via polymeric nanoparticles. *J. Controlled Release* **2015**, *219*, 488−499.
(8) Fröhlich, E. The role of surface charge in cellular uptake and cytotoxicity of medical nanoparticles. *Int. J. Nanomed.* **2012**, *7*, 5577−5591.
(9) Jager, M.; Schubert, S.; Ochrimenko, S.; Fischer, D.; Schubert, U. S. Branched and linear poly(ethylene imine)-based conjugates: synthetic modification, characterization, and application. *Chem. Soc. Rev.* **2012**, *41*, 4755−67.
(10) Akinc, A.; Thomas, M.; Klibanov, A. M.; Langer, R. Exploring polyethylenimine-mediated DNA transfection and the proton sponge hypothesis. *J. Gene Med.* **2005**, *7*, 657−63.
(11) Gao, X.; Yao, L.; Song, Q.; Zhu, L.; Xia, Z.; Xia, H.; Jiang, X.; Chen, J.; Chen, H. The association of autophagy with polyethylenimine-induced cytotoxicity in nephritic and hepatic cell lines. *Biomaterials* **2011**, *32*, 8613−25.
(12) Kafil, V.; Omidi, Y. Cytotoxic impacts of linear and branched polyethylenimine nanostructures in a431 cells. *BioImpacts* **2011**, *1*, 23−30.
(13) Lv, H.; Zhang, S.; Wang, B.; Cui, S.; Yan, J. Toxicity of cationic lipids and cationic polymers in gene delivery. *J. Controlled Release* **2006**, *114*, 100−9.
(14) Islam, M. A.; Park, T. E.; Singh, B.; Maharjan, S.; Firdous, J.; Cho, M. H.; Kang, S. K.; Yun, C. H.; Choi, Y. J.; Cho, C. S. Major degradable polycations as carriers for DNA and siRNA. *J. Controlled Release* **2014**, *193*, 74−89.
(15) Wang, W.; Naolou, T.; Ma, N.; Deng, Z.; Xu, X.; Mansfeld, U.; Wischke, C.; Gossen, M.; Neffe, A. T.; Lendlein, A. Polydepsipeptide Block-Stabilized Polyplexes for Efficient Transfection of Primary Human Cells. *Biomacromolecules* **2017**, *18*, 3819−3833.
(16) Lungu, C. N.; Diudea, M. V.; Putz, M. V.; Grudzinski, I. P. Linear and Branched PEIs (Polyethylenimines) and Their Property Space. *Int. J. Mol. Sci.* **2016**, *17*, 555.
(17) Cui, J.; Qin, L.; Zhang, J.; Abrahimi, P.; Li, H.; Li, G.; Tietjen, G. T.; Tellides, G.; Pober, J. S.; Saltzman, W. M. Ex vivo pretreatment of human vessels with siRNA nanoparticles provides protein silencing in endothelial cells. *Nat. Commun.* **2017**, *8*, 191.
(18) Jiang, Y.; Gaudin, A.; Zhang, J.; Agarwal, T.; Song, E.; Kauffman, A. C.; Tietjen, G. T.; Wang, Y.; Jiang, Z.; Cheng, C. J.; Saltzman, W. M. A "top-down" approach to actuate poly(amine-co-ester) terpolymers for potent and safe mRNA delivery. *Biomaterials* **2018**, *176*, 122−130.
(19) Adams, B. D.; Wali, V. B.; Cheng, C. J.; Inukai, S.; Booth, C. J.; Agarwal, S.; Rimm, D. L.; Gyorffy, B.; Santarpia, L.; Pusztai, L.; Saltzman, W. M.; Slack, F. J. miR-34a Silences c-SRC to Attenuate Tumor Growth in Triple-Negative Breast Cancer. *Cancer Res.* **2016**, *76*, 927−39.
(20) Piest, M.; Engbersen, J. F. Effects of charge density and hydrophobicity of poly(amido amine)s for non-viral gene delivery. *J. Controlled Release* **2010**, *148*, 83−90.
(21) Kuhn, P. S.; Levin, Y.; Barbosa, M. C. Charge inversion in DNA−amphiphile complexes: possible application to gene therapy. *Phys. A* **1999**, *274*, 8−18.
(22) McCall, R. L.; Sirianni, R. W. PLGA Nanoparticles Formed by Single- or Double-emulsion with Vitamin E-TPGS. *J. Visualized Exp.* **2013**, 51015.
(23) Repetto, G.; del Peso, A.; Zurita, J. L. Neutral red uptake assay for the estimation of cell viability/cytotoxicity. *Nat. Protoc.* **2008**, *3*, 1125.
(24) Zhang, X.; Tang, W.; Yang, Z.; Luo, X.; Luo, H.; Gao, D.; Chen, Y.; Jiang, Q.; Liu, J.; Jiang, Z. PEGylated poly(amine-co-ester) micelles as biodegradable non-viral gene vectors with enhanced stability, reduced toxicity and higher in vivo transfection efficacy. *J. Mater. Chem. B* **2014**, *2*, 4034−4044.
(25) Jiang, Z. Lipase-Catalyzed Synthesis of Poly(amine-co-esters) via Copolymerization of Diester with Amino-Substituted Diol. *Biomacromolecules* **2010**, *11*, 1089−1093.
(26) Liu, J.; Jiang, Z.; Zhou, J.; Zhang, S.; Saltzman, W. M. Enzyme-synthesized poly(amine-co-esters) as nonviral vectors for gene delivery. *J. Biomed. Mater. Res., Part A* **2011**, *96*, 456−65.
(27) Voevodina, I.; Scandola, M.; Zhang, J.; Jiang, Z. Exploring the Solid State Properties of Enzymatic Poly(amine-co-ester) Terpolymers to Expand their Applications in Gene Transfection. *RSC Adv.* **2014**, *4*, 8953−8961.
(28) Hacker, M. C.; Mikos, A. G. Synthetic Polymers. In *Principles of Regenerative Medicine*, 2nd ed.; Atala, A., Lanza, R., Thomson, J. A., Nerem, R., Eds.; Elsevier Academic Press: San Diego, CA, 2011; Chapter 33, pp 587−622.
(29) Mok, M. M.; Kim, J.; Torkelson, J. M. Gradient copolymers with broad glass transition temperature regions: Design of purely interphase compositions for damping applications. *J. Polym. Sci., Part B: Polym. Phys.* **2008**, *46*, 48−58.
(30) Goodfriend, A. C.; Welch, T. R.; Nguyen, K. T.; Johnson, R. F.; Sebastian, V.; Reddy, S. V.; Forbess, J.; Nugent, A. Thermally processed polymeric microparticles for year-long delivery of dexamethasone. *Mater. Sci. Eng., C* **2016**, *58*, 595−600.
(31) Jasinski, F.; Teo, V. L.; Kuchel, R. P.; Mballa Mballa, M.; Thickett, S. C.; Brinkhuis, R. H. G.; Weaver, W.; Zetterlund, P. B. Synthesis and characterisation of gradient polymeric nanoparticles. *Polym. Chem.* **2017**, *8*, 495−499.
(32) Zhang, X.; Liu, B.; Yang, Z.; Zhang, C.; Li, H.; Luo, X.; Luo, H.; Gao, D.; Jiang, Q.; Liu, J.; Jiang, Z. Micelles of enzymatically synthesized PEG-poly(amine-co-ester) block copolymers as pH-responsive nanocarriers for docetaxel delivery. *Colloids Surf., B* **2014**, *115*, 349−58.
(33) Wang, X.; Lian, K.; Chen, T. Experiment Research on Bonding Effect of Poly(lactic-co-glycolic acid) Device by Surface Treatment Method. *Int. J. Polym. Sci.* **2015**, *2015*, 1−7.
(34) Agrawal, G.; Negi, Y. S.; Pradhan, S.; Dash, M.; Samal, S. K., Wettability and contact angle of polymeric biomaterials. In *Characterization of Polymeric Biomaterials*, Tanzi, M. C., Farè, S., Eds.; Woodhead Publishing: 2017; Chapter 3, pp 57−81.
(35) Mohiti-Asli, M.; Saha, S.; Murphy, S. V.; Gracz, H.; Pourdeyhimi, B.; Atala, A.; Loboa, E. G. Ibuprofen loaded PLA nanofibrous scaffolds increase proliferation of human skin cells in vitro and promote healing of full thickness incision wounds in vivo. *J. Biomed. Mater. Res., Part B* **2017**, *105*, 327−339.
(36) Saltzman, W. M.; Kyriakides, T. R. Cell Interactions with Polymers. In *Principles of Tissue Engineering*, 4th ed.; Lanza, R., Langer, R., Vacanti, J., Eds.; Academic Press: Boston, 2014; Chapter 20, pp 385−406.
(37) Mislick, K. A.; Baldeschwieler, J. D. Evidence for the role of proteoglycans in cation-mediated gene transfer. *Proc. Natl. Acad. Sci. U. S. A.* **1996**, *93*, 12349−54.
(38) Zhang, J.; Cui, J.; Deng, Y.; Jiang, Z.; Saltzman, W. M. Multifunctional Poly(amine-co-ester-co-orthoester) for Efficient and Safe Gene Delivery. *ACS Biomater. Sci. Eng.* **2016**, *2*, 2080−2089.
(39) Ahn, S.; Seo, E.; Kim, K.; Lee, S. J. Controlled cellular uptake and drug efficacy of nanotherapeutics. *Sci. Rep.* **2013**, *3*, 1997.
(40) Avci-Adali, M.; Behring, A.; Keller, T.; Krajewski, S.; Schlensak, C.; Wendel, H. P. Optimized conditions for successful transfection of human endothelial cells with in vitro synthesized and modified mRNA for induction of protein expression. *J. Biol. Eng.* **2014**, *8*, 8−8.
(41) Martin, D. T.; Steinbach, J. M.; Liu, J.; Shimizu, S.; Kaimakliotis, H. Z.; Wheeler, M. A.; Hittelman, A. B.; Mark Saltzman, W.; Weiss, R. M. Surface-modified nanoparticles enhance transurothelial penetration and delivery of survivin siRNA in treating bladder cancer. *Mol. Cancer Ther.* **2014**, *13*, 71−81.

DOI: 10.1021/acs.biomac.8b00997
Biomacromolecules 2018, 19, 3861−3873